Electronic structure and heavy-fermion behavior in LiV_2O_4

D. J. Singh
Code 6391, Naval Research Laboratory, Washington, DC 20375

P. Blaha and K. Schwarz
Institut für Physik und Theoretische Cheme, TU Wien, A-1060 Wien, Austria

I. I. Mazin
Code 6391, Naval Research Laboratory, Washington, DC 20375

(Received 14 July 1999)

First principles density functional calculations of the electronic and magnetic properties of spinel-structure LiV_2O_4 have been performed using the full potential linearized augmented plane-wave method. The calculations show that the electronic structure near the Fermi energy consists of a manifold of 12 bands derived from V t_{2g} states, weakly hybridized with O p states. While the total width of this active manifold is approximately 2 eV, it may be roughly decomposed into two groups: high velocity bands and flatter bands, although these mix in density functional calculations. The flat bands, which are the more atomiclike, lead to a high density of states and magnetic instability of local moment character. The value of the on-site exchange energy is sensitive to the exact exchange correlation parametrization used in the calculations, but is much larger than the interaction between neighboring spins, reflecting the weak coupling of the magnetic system with the high velocity bands. A scenario for the observed heavy-fermion behavior is discussed, in which conduction electrons in the dispersive bands are weakly scattered by local moments associated with strongly correlated electrons in the heavy bands. This is analogous to that in conventional Kondo-type heavy fermions, but is unusual in that both the local moments and conduction electrons come from the same d manifold. [S0163-1829(99)00548-2]

I. INTRODUCTION

Heavy-fermion (HF) materials are typically intermetallic compounds containing Ce, U, or Yb atoms. They are characterized by the usual Landau Fermi liquid scaling properties, but only at very low temperatures (beginning as low as 0.3 K, depending on the material) and with extraordinarily strongly renormalized effective masses, $m^* \approx 100 - 1000 m_e$.[1–3] They show apparent local moment paramagnetic behavior with strongly increasing spin susceptibility, χ, and specific heat coefficient γ with decreasing temperature, but do not order magnetically, and eventually settle at low T into a state with constant γ and χ and Wilson ratio near unity. Following extensive investigation over many years, a basic understanding of the phenomena has been established. The origin is a many body effect associated with the interaction of itinerant conduction electrons with strongly correlated f electrons on local moment rare earth ions. Thus, the discovery by Kondo and co-workers of HF behavior[4] with $\gamma \approx 0.42$ J/mol K^2, in the transition metal oxide LiV_2O_4, was both remarkable and unexpected, as the material does not appear to fit into this framework.

As may be expected, this discovery has led to a series of detailed experiments that have confirmed the original result with properties characteristic of the heaviest f-electron HF materials,[5–10] although it should be noted that Fujiwara and co-workers proposed an alternate explanation of their NMR data within a spin-fluctuation framework.[7]

Two first principles band structure calculations have recently appeared,[11,12] though both use spherical approximations for the potential. These reasonably agree with each other but not as well with the full potential calculations presented here. Their conclusions are, however, different: Eyert *et al.*[11] suggest that LiV_2O_4 is not a ''true'' HF material in the sense that they ascribe the specific heat enhancement to spin fluctuations arising from frustrated antiferromagnetism on the V sublattice; Anisimov *et al.*[12] advocate a separation of V d electrons into two sets, a localized and an itinerant one, playing the role of the f and conduction electrons in conventional HF materials. A related model is discussed by Varma.[13] We argue that the true HF picture is likely, since it is compatible with the electronic structure obtained and is consistent with the experimental situation. Very recently, another full potential electronic structure calculation has also appeared, reporting non-spin-polarized band structures that agree with the present ones, though with quite different conclusions.[14]

LiV_2O_4 occurs in an undistorted cubic fcc spinel structure, as shown in Fig. 1. The $V^{3.5+}$ ($3d1.5$) ions are located in very slightly distorted O octahedra. These V ions form corner-sharing tetrahedra ordered on the fcc lattice, such that each V has six neighbors of the same kind. Thus, the V sublattice can be viewed as an fcc lattice with every second atom removed. Alternately, it can be viewed as a collection of chains running along all the (110)-type directions with each V participating in three chains. This structure leads to strong geometric frustration of antiferromagnetic (AF) interactions, although of course ferromagnetic (FM) interactions are unfrustrated. As noted, LiV_2O_4 is paramagnetic at low temperature. However, Krimmel and co-workers[10] have reported quasielastic neutron scattering measurements, that show predominantly FM fluctuations above 40 K with sub-

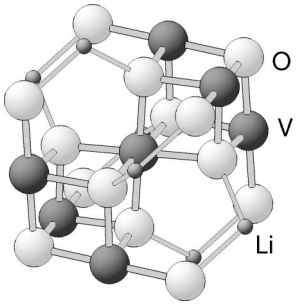

FIG. 1. Structure of LiV_2O_4 showing the local coordination of a V atom. Note that the central V in the figure is at the center of an O octahedron oriented along the 100 axes and on the joint vertex of two corner-sharing V tetrahedra, leading to the rhombohedral site symmetry.

stantial observable AFM fluctuations only at lower temperatures, where they significantly contribute to the spectra.

II. BAND STRUCTURE AND MAGNETISM

In this structural configuration, we find that the O $2p$ bands are below and well separated from the transition metal derived bands, so that both the Li-O and V-O bonds are strongly ionic. The higher lying $3d$ derived orbitals are crystal field split into a sixfold degenerate (three per spin) t_{2g} manifold and a higher lying fourfold degenerate e_g manifold. Neither the crystal structure nor the electronic configuration is particularly favorable for substantial V $3d$–O $2p$ hybridization, so narrow d bands are obtained with clean crystal field gaps between the t_{2g} and e_g manifolds. We do not get noticeable mixing of these manifolds. Thus, the electronic structure relevant to low energy excitations may be described as a manifold of 12 narrow t_{2g} bands 1/4 filled with 6 electrons (note that there are 4 V ions per cell) with no other nearby bands. Much of the bandwidth is due to direct V-V hopping. At first glance it is hard to recognize the connection between this electronic structure and that of the *f*-electron HF compounds.

We find, using density functional calculations with the full potential linearized augmented planewave (LAPW) method,[15–18] that the t_{2g} manifold in fact contains two different types of carriers, as was also emphasized by Anisimov *et al.*[12] Calculations with the tight-binding linear muffin tin orbitals (TB-LMTO) method[19] were used to analyze the band symmetries. One carrier type is analogous to the itinerant conduction electrons of conventional HF materials and the others can play the role of the strongly correlated local moment *f* electrons. This provides a way of obtaining conventional HF behavior in LiV_2O_4, albeit in an unconventional way, at least as regards the nature of the bare states.

The calculated local spin density approximation (LSDA) band structure for non-spin-polarized (NSP) LiV_2O_4 is shown in Fig. 2. The corresponding electronic density of states is given in Fig. 3. The O $2p$ bands span the range from approximately -8 to -3 eV (relative to E_F). The $12t_{2g}$ bands are separated from these by a gap and have a width of slightly less than 2.5 eV. The e_g manifold is quite narrow, characteristic of the bonding topology of spinels, which features bent V-O-V bonds, unfavorable for band formation via $e_g - p\sigma$ hybridization. These are again well separated from

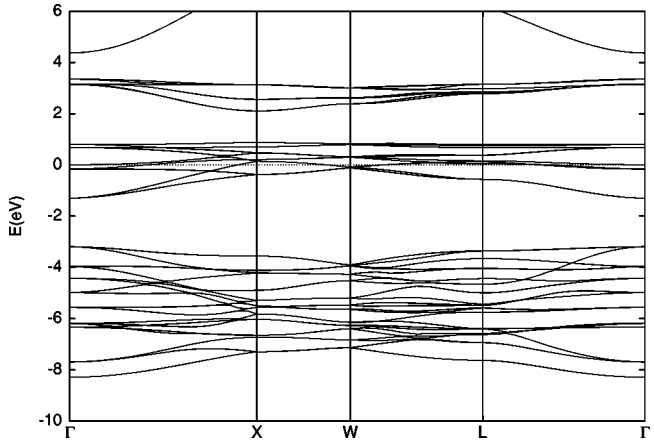

FIG. 2. Calculated band structure of non-spin-polarized LiV_2O_4. The Fermi energy is denoted by the dashed horizontal line at 0.

the active t_{2g} bands by a gap of slightly less than 1.5 eV. The dispersion of the t_{2g} bands is in fact mostly derived from V-V hopping as was verified by removing the O orbitals from TB-LMTO calculations. A blow-up of the band structure showing the t_{2g} bands, which dominate the low energy physics, is given in Fig. 4. Although a high on-site Coulomb repulsion, U, is not expected in early $3d$ compounds like this, significant correlation effects on this band structure should not be excluded since the active manifold is narrow. Photoemission measurements[20] imply $U \approx 2$ eV, which is comparable to the bandwidth, and therefore consistent with at least moderate correlation effects in this multiband system.

Spin polarized calculations, also using the full potential LAPW method, both within the LSDA and with generalized gradient approximations (GGA)[21] show a considerable magnetic instability, of strong local moment character. Calculations were done for ferromagnetic, antiferromagnetic (AF: 2 of 4 spins flipped per unit cell) and ferrimagnetic (FiM: 1 of 4 spins flipped) configurations. Very low Hellman-Feynman forces on the symmetry unconstrained O coordinates were obtained in the experimental crystal structure, used in these calculations, independent of the magnetic order, supporting the experimental structure and implying only weak magne-

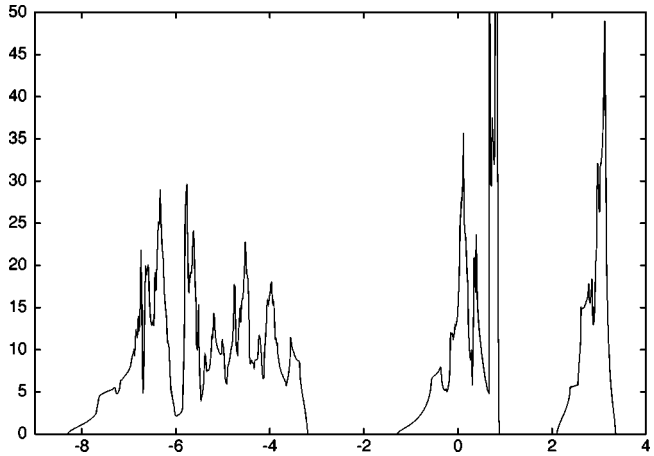

FIG. 3. Electronic density of states of non-spin-polarized LiV_2O_4 in states per eV, per unit cell (4 V atoms) as a function of energy in eV. The Fermi energy is at 0.

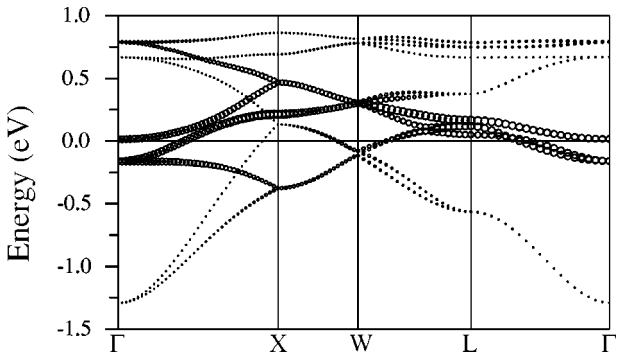

FIG. 4. Calculated band structure of non-spin-polarized LiV_2O_4, showing the t_{2g} manifold. The sizes of the points denote the calculated relative amounts of the a_{1g} character in the states. The Fermi energy is denoted by the dashed horizontal line at 0.

toelastic effects, as may have been anticipated based on the weakly hybridized electronic structure. Within the LSDA, a FM spin polarization of 1.15 μ_B/V with an energy 60 meV/V below the NSP energy is obtained. The AF and FiM energies were both 5 meV/V lower than the FM. This is qualitatively different from the results of Eyert *et al.*,[11] who found energies and moments closer to an itinerant magnetic system, consistent with strong scattering of carriers by spin fluctuations at the LSDA level.

The GGA results are qualitatively similar to the LSDA, but are somewhat more magnetic. In the GGA, the FM spin polarization is increased to 1.4 μ_B/V, which is a greater than usual sensitivity to the exchange correlation functional. The magnetic properties are also unusually sensitive to other details of the calculations. For instance, the atomic sphere approximation (ASA), used in Refs. 11 and 12, as well as in our LMTO calculations, leads to a substantial underestimate of the magnetic moment, namely 0.5 μ_B/V, compared with our full potential LAPW calculations. This is also unusual and calls for caution when using ASA calculations for quantitative estimates of the electronic parameters (cf. Ref. 12). This is related to the physics discussed below. First of all, the magnetization comes almost entirely from one *d* submanifold, resulting in a highly nonspherical exchange potential, which is spherically averaged in non-full-potential calculations, reducing its effect. Secondly, the NSP energy bands differ, such that the full-potential band structure has higher values of the density of states around the Fermi level, and therefore a stronger Stoner instability. To test this, extended Stoner calculations were performed with the same Stoner *I* (from the TB-LMTO), but with the LSDA TB-LMTO and LAPW densities of states. This gave a FM magnetization of slightly more than 0.5 and slightly more than 1 μ_B/V, respectively, indicating that the changes in the bare NSP bands are the more important factor, although it should be noted that with the full exchange splitting, the bands are nonrigid, so the extended Stoner is not fully valid and the result should be regarded as qualitative.

The calculated spin density (Fig. 5) is remarkable, in that, despite the nearly cubic environment, it strongly reflects the weak rhombohedral symmetry. This is a result of the fact that the hopping that gives rise to the t_{2g} dispersions is largely V-V and that the V neighbors are a rhombohedral environment. The primary pseudocubic quantization axis is

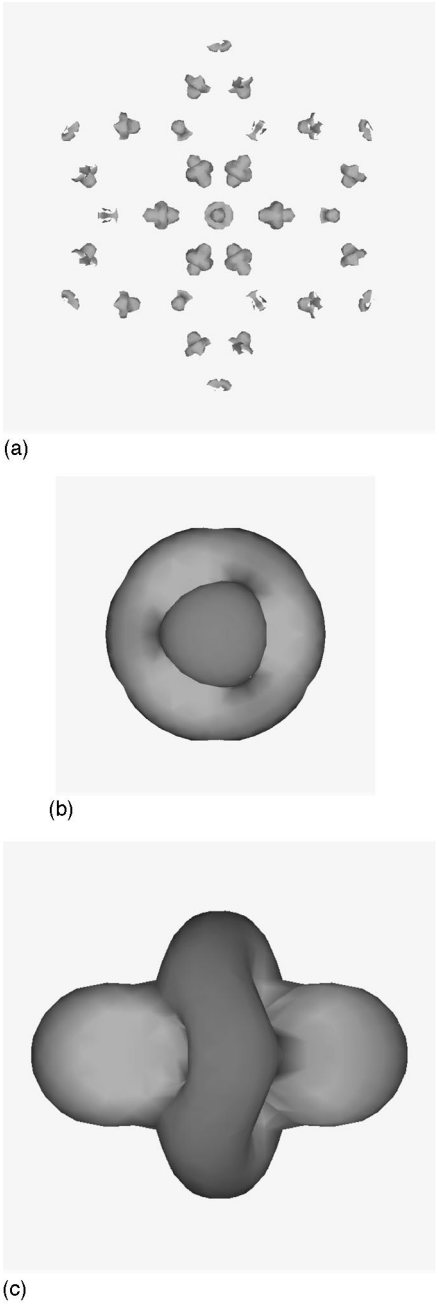

FIG. 5. Calculated spin density of LiV_2O_4 with a ferromagnetic ordering. The top panel shows an 0.1 μ_B/a.u.^{3} isosurface viewed along a 111 direction, the middle is the same view blown up around a single V ion, while the bottom panel is the same on a -110. Note the predominant but not pure a_{1g} character. The small e_g' admixture is responsible for the triangular rather than full symmetry viewed from the top (middle panel) and the buckling of the central ''doughnut'' in the side view (bottom panel).

along the Cartesian 100 directions, because of the octahedral mostly O derived crystal field that splits the t_{2g} and e_g manifolds. In the rhombohedral site symmetry, there is a further quantization of the t_{2g} space based on the rhombohedral 111 axis, into a double degenerate e_g space and a single degenerate a_{1g} manifold. In order to distinguish this e_g from the higher lying e_g manifold split off by the octahedral crystal field, we will denote it as e_g' in the following. The e_g' and a_{1g} are at the same energy in LiV_2O_4 but are locally orthogonal

spaces. The remarkable result, evident in Fig. 5, is that the magnetization is derived almost entirely from the a_{1g} subspace.

We obtain almost complete polarization of the relevant a_{1g} submanifold in our full-potential LSDA and GGA calculations. Besides the higher resulting magnetic moments, we obtain much clearer strong local moment behavior in these calculations. The V moments as characterized by integrated spin magnetization in the V LAPW spheres for the AF and FiM cases are within 9% of the FM value. The FiM and AF cases were energetically degenerate to within the accuracy of the calculations at 5 meV/V below the FM energy, consistent with weak AF exchange interactions and magnetism that, as noted above, is very strongly local moment in character.

As mentioned, the dispersion of the t_{2g} bands is nearly exclusively derived from the V-V interaction. This includes the nearest neighbor $dd\sigma$ and $dd\pi$ hoppings. Inverting the TB-LMTO Hamiltonian, we get a rough estimate, $t_{dd\sigma}/t_{dd\pi} \sim 3.5$ (and $t_{dd\delta} \ll t_{dd\pi}$). The 12×12 TB Hamiltonian in this case is defined by the overlap integrals for each V-V bond, e.g., for the (110) bond $t_{xy-xy}=\frac{3}{4}t_{dd\sigma}$, $t_{yz-xz}=t_{dd\pi}$, $t_{xy-xz}=0$. An interesting property of this Hamiltonian is that when $t_{dd\sigma}=\frac{8}{3}t_{dd\pi}$, two bands are flat. These bands are nonbonding combinations of e_g' states of the four V ions. In actual calculations, this condition is satisfied only very approximately (within $\approx$40 percent), but the corresponding states are still very flat (the width is 0.2 eV) and located about 0.8 eV above the Fermi level. Full-potential LAPW calculations reveal also two more relatively flat bands of the e_g' character right below these, but still about 0.7 eV above the Fermi level. On the other hand, a closer look reveals four more heavy bands (width $\approx$0.5 eV) that are located around the Fermi level. Those have predominantly a_{1g} character and give rise to the high concentration of a_{1g} character around E_F, and the high density of states in the same region with the resulting magnetic instability (cf. Fig. 4). The remaining bands are mixed in the LSDA; e_g' character dominates and they have greater dispersion.

III. SCENARIO FOR HEAVY-FERMION BEHAVIOR

The variation of the effective mass is substantial: near the bottom of the t_{2g} manifold, it is close to the free electron mass (which is unusually small for *d* bands), while near the Fermi level it is 4–5. From the transport point of view, one can speak about two groups of carriers: four light bands (comparable with the *sp* bands in transition metals), and four heavier bands (with their width of $\approx$0.5 eV). Additionally, there are four flat bands at about 0.7–0.8 eV above E_F. The bands providing the heavy carriers like the light bands (width 2 eV) cross the Fermi level but are responsible for the calculated local moment magnetic instability. These heavy bands near E_F are dominated by a_{1g} character, while the remainder of the bands, although mixed are dominated by e_g' character.

In the scenario proposed here, the states relevant to the transport properties are from the heavy and light bands near E_F; these may constitute the two classes of carriers mentioned above. This connects with conventional HF materials, in that LSDA calculations for these materials also show band structures consisting of broader conduction bands and narrow ($W \ll U$) bands at E_F associated with local moments. In conventional HF materials, these two classes of bands are coupled, but weakly. The first evidence for this in LiV_2O_4 is through the small (but no doubt overestimated in LSDA) interatomic exchange interactions, as seen by the near degeneracy of the various magnetic configurations studied and the fact that although the ferromagnetic band structure has exchange splittings in all bands, very little polarization of the e_g' orbitals is induced as discussed above. Further, more clear signatures emerge from the transport functions, particularly $N(E_F)\langle v_F^2\rangle \propto V\omega_p^2 \propto V(n/m)$, where v_F is the band velocity on the Fermi surface, V is the unit cell volume, ω_p is the plasma frequency, n/m is the optical n/m, and the average $\langle\ \rangle$ is over the Fermi surface. This function is dominated by more dispersive bands due to the $\langle v_F^2\rangle$ factor, so that changes with magnetic order are reflective of the interaction between the low dispersion states responsible for the magnetism and the more dispersive conduction a_{1g} derived bands. We obtain $N(E_F)$ of 7.26 eV^{-1} on a per formula unit basis (2 V atoms) for the paramagnetic calculation, and 7.23 eV^{-1} for the FM majority spin channel, 1.58 eV^{-1} for the FM minority channel, 2.96 eV^{-1} for the FiM majority spin channel, and 7.24 eV^{-1} for the FiM minority channel. The corresponding Fermi velocities (cm/s) are 0.77×10^7, 0.30×10^7, 1.37×10^7, 0.60×10^7, and 0.75×10^7. The LSDA values of $N(E_F)\langle v_F^2\rangle$ stay within 20% of the paramagnetic value.

So far, all our results emerge from first principles density functional calculations primarily within the LSDA, using the full potential LAPW method. This includes the separation into two different types of carriers, a_{1g}-like and e_g'-like, and the strongly spin polarized a_{1g}-like local moment magnetism. Coulomb correlations as included approximately in the LSDA+U method are not required. This is of some significance, because in the LMTO calculations of Ref. 12 a U of 3 eV was used to obtain these, and this U is about 50% greater than the value implied by photoemission, and is also a value that would split the e_g' space into strongly correlated upper and lower Hubbard bands. On the other hand, with the screened U less than or equal to the value indicated by photoemission, as is normal, i.e., $U \lesssim 2$ eV, the light e_g' derived bands would be weakly to moderately correlated and metallic as in conventional HF, while only the heavy a_{1g} bands would be strongly correlated. In fact, the actual situation may be more complicated, because the two relevant types of carriers are derived from the same *d* manifold and therefore may be more strongly coupled than in conventional HF, as discussed below.

IV. DISCUSSION

Even in weakly correlated materials, LSDA calculations overestimate the extent of hybridization between different orbitals. Thus one may anticipate the following artifacts in the LSDA calculations: (1) the heavy a_{1g} bands could be narrower than calculated; (2) the mixture between a_{1g} and e_g' bands could be weaker than calculated; (3) as a result, the dominance of a_{1g} character in the spin density could be stronger than that obtained from the LSDA. This is like the corresponding artifacts in band calculations for *f* band metals where the hybridization of the *f* bands with the conduction

bands is overestimated in the LSDA. These are partially local effects related to LSDA errors in the description of the bonding and not directly related to Hubbard-type correlations controlled by U/W (the same effects are present in wide band materials, where, for example, LSDA estimates of interatomic magnetic couplings, J, are often overestimated). Additionally, the effect of Hubbard-type correlations, which are neglected in band structure calculations, may be expected to be strong for the heavy mass carriers, since taking $U \lesssim 2$ eV, as indicated by photoemission measurements,[20] yields $U/W \lesssim 4$. At such values of U/W, one may expect a substantial suppression of charge fluctuations involving the heavy mass bands along the lines of the normal f electron HF systems. However, the real situation is undoubtably considerably more complex, as some Hubbard correlation effects may be present in the bare light carrier bands where $U/W \lesssim 1$, and exceptionally strong off-diagonal Hubbard effects may be expected as well, since the relevant bands (heavy and light) are both derived from the V t_{2g} space. It will be quite interesting to construct and study many body models of this type in the HF regime. Only the t_{2g} orbitals and the interactions among them should be needed. There should be four light bands and four related flat bands away from E_F per unit cell. These should be formed from two orbitals per V using V-V hopping, as described in the tight binding discussion above. The light bands, which provide the carriers, should have a width of 2 eV, $U/W \lesssim 1$, and contain ≈ 0.5 electrons per V. In addition, there should be a localized set of atomiclike orbitals (one per V) with occupation $1e$ and bare band width ≈ 0.5 eV. Additionally, the off-diagonal Coulomb repulsion coupling these two groups of states should be comparable, i.e., ≈ 2 eV. LiV_2O_4 can be made quite cleanly and is well suited to detailed experimental investigation, and this may make it an especially interesting system for experimental and theoretical study.

ACKNOWLEDGMENTS

Computations were performed using facilities of the DoD HPCMO ASC and NAVO Centers. Work at the Naval Research Laboratory was supported by the Office of Naval Research.

[1] K. Anders, J.E. Graebner, and H.R. Ott, Phys. Rev. Lett. **35**, 1779 (1975).
[2] G.R. Stewart, Rev. Mod. Phys. **56**, 755 (1984).
[3] G. Aeppli and Z. Fisk, Comments Condens. Matter Phys. **16**, 155 (1992).
[4] S. Kondo, D.C. Johnston, C.A. Swenson, F. Borsa, A.V. Mahajan, L.L. Miller, T. Gu, A.I. Goldman, M.B. Maple, D.A. Gajewski, E.J. Freeman, N.R. Dilley, R.P. Dickey, J. Merrin, K. Kojima, G.M. Luke, Y.J. Uemura, O. Chmaissem, and J.D. Jorgensen, Phys. Rev. Lett. **78**, 3729 (1997).
[5] O. Chmaissem, J.D. Jorgensen, S. Kondo, and D.C. Johnston, Phys. Rev. Lett. **79**, 4886 (1997).
[6] A.V. Mahajan, R. Sala, E. Lee, F. Borsa, S. Kondo, and D.C. Johnston, Phys. Rev. B **57**, 8890 (1998).
[7] N. Fujiwara, H. Yasuoka, and Y. Ueda, Phys. Rev. B **57**, 3539 (1998).
[8] S. Kondo, D.C. Johnston, and L.L. Miller, Phys. Rev. B **59**, 2609 (1999).
[9] D.C. Johnston, C.A. Swenson, and S. Kondo, Phys. Rev. B **59**, 2627 (1999).
[10] A. Krimmel, A. Loidl, M. Klemm, S. Horn, and H. Schober, Phys. Rev. Lett. **82**, 2919 (1999).
[11] V. Eyert, K.H. Hock, S. Horn, A. Loidl, and P.S. Riseborough, Europhys. Lett. **46**, 762 (1999).
[12] V.I. Anisimov, M.A. Korotin, M. Zolfl, T. Pruschke, K. Le Hur, and T.M. Rice, Phys. Rev. Lett. **83**, 364 (1999).
[13] C. M. Varma, Phys. Rev. B **60**, 6973 (1999).
[14] J. Matsuno, A. Fujimori, and L.F. Mattheiss, Phys. Rev. B **60**, 1607 (1999).
[15] D. J. Singh, *Planewaves, Pseudopotentials and the LAPW Method* (Kluwer Academic, Boston, 1994).
[16] Highly converged calculations were performed with two separate codes, WIEN97 (Ref. 17), and an independent general potential LAPW code (Ref. 18), using different choices of sphere radii, zone integration, and other parameters. No significant differences were found in parallel calculations.
[17] P. Blaha, K. Schwarz, and J. Luitz, Vienna University of Technology, 1997 [Improved and updated Unix version of the WIEN code, published by P. Blaha, K. Schwarz, P. Sorantin, and S. B. Trickey, Comput. Phys. Commun. **59**, 399 (1990)].
[18] S.H. Wei and H. Krakauer, Phys. Rev. Lett. **55**, 1200 (1985); D. Singh, Phys. Rev. B **43**, 6388 (1991).
[19] O.K. Andersen, Phys. Rev. B **12**, 3060 (1975); O.K. Andersen and O. Jepsen, Phys. Rev. Lett. **53**, 2571 (1984).
[20] A. Fujimori, K. Kawakami, and N. Tsuda, Phys. Rev. B **38**, 7889 (1998).
[21] J.P. Perdew, K. Burke, and M. Ernzerhof, Phys. Rev. Lett. **78**, 1396 (1996); **78**, 1396 (1997) (E).